Effect of different dispersing agents in the non-isothermal kinetics and thermomechanical behaviour of PET/TiO_2 composites

D. Cayuela [(1)], M. Cot [(2)], I. Algaba [(3)], A.M. Manich [(4)]

(1) Textile Research Institute (INTEXTER), Technical University of Catalonia (UPC), Spain.
(2) Department of Textile and Paper Engineering (DETIP), Technical University of Catalonia (UPC), Spain.
(3) Department of Statistics and Operations Research (EIO), Technical University of Catalonia (UPC), Spain.
(4) Institute of Advanced Chemistry of Catalonia (IQAC), Spanish National Research Council, (CSIC), Spain.

Abstract

This work is based on the analysis of the influence of dispersing agents on the non-isothermal kinetics, thermomechanical behaviour and dispersing action of PET/TiO_2 nanocomposites. The influence of two montanic waxes and an amide wax used as dispersing agents in the nucleating effect of the nanoparticles is studied. The dispersing agents are the following: a) a partly saponified ester of montanic acids (PSEMA), b) an ester of montanic acids with multifunctional alcohols (MAWMA) and c) an amide wax based on N,N'-Bisstearoyl ethylenediamine (AW). The non-isothermal kinetics based on the Avrami method revealed that MAWMA and PSEMA favours the nucleating effect of the nanoparticles when are included in PET. Birefringence microscopy points out the good dispersing capacity of MAWMA and AW and the termomechanical analysis confirmed that the ester of montanic acids with multifunctional alcohols MAWMA shows the best dispersing properties and best promotes the nucleating effect of the TiO_2 nanoparticles when used for PET/TiO_2 nanocomposites production.

Keywords: TiO_2 nanoparticles, PET/TiO_2 nanocomposites, amide wax, montanic wax, dispersing agent, non-isothermal kinetics, termomechanical analysis, nucleating effect.

INTRODUCTION

Ceramic nanoparticles are inorganic substances with high chemical and thermal resistance. They are very attractive to be used as fillers in polymeric nanocomposites, because they can be easily obtained at relatively low cost, resulting in a very desirable structure of layers.

Most of the applications of ceramic nanoparticles in polymeric matrix are directed to the formation of films or substrates produced by injection or molding. Composite materials in filament form are much more limited and their structure and properties are very different from those of a film. In fact, functional fibres will be one of the key factors for the survival of the textile industry being of particular interest those containing ceramics (1). Depending on the applied ceramic, different functional fibres can be obtained. If TiO_2 is included into the fibre, UV protective characteristics are obtained. Their photo- catalytic properties enabled them to absorb the UV radiation and provide antibacterial barriers. The non-toxicity, chemical stability at high temperatures, and permanent stability under UV rays makes them very attractive in a wide range of applications.

The production of nanocomposite filaments needs a previous study on the compatibility of the polymer/nanoparticle systems in order to enhance the bonds between matrix and nanoparticles, due to the imposed technical specifications that include tensile and abrasion requirements, resistance to ageing, washing, and weathering fastness, etc.

When nanoparticles are added in the mass of the fibre, the major challenge is the adequate dispersion of nanoparticles into the polymer to prevent their aggregation. Among the possible methods to introduce nanoparticles in the fibres (2, 3, 4, 5, 6, 7, 8), the melt-blending process is the more commercially attractive due to its versatility, although agglomeration of nanoparticles can occur. To prevent agglomeration, the surface of the nanoparticles can be modified through bonding organic components on its surface, yielding anchorage or bonding capacity with the polymer (9), or including a dispersing agent in the mixture.

In a previous work, the authors studied the effect of surface treatment of TiO_2 with tri-n-octylphosphine oxide (TOPO) on its compatibility when included as filler in poly(ethylene terephthalate) (10). It was shown that the surface treatment and the concentration of nanofiller influence the non-isothermal crystallization behaviour, the viscoelastic transitions and the cold crystallization of the PET nanocomposites and optimal conditions of compatibility and nucleation were determined.

With regards to the dispersing agents, some of them, based on esther of montanic acids with multifunctional alcohols and a partly saponified ester wax for polyester processing (11), present a nucleating effect and excellent release and flow properties, although their effect on the dispersion of ceramic particles when included in PET for composite formation has not been studied. The montanic esters used in this study are secondary products of the oxidative refining of raw montan wax. The montanic acids contained in raw montan wax are straightchain, unbranched monocarboxylic acids with a chain length in the range of C28-C32. As a result of the long chain these montanic acids have an high thermo stability and a low volatility.

The amide wax (AW) based on N, N'-bisstearoylethylenediamine presents increased thermo

stability. Due to its low volatility, this dispersing agent is used in engineering plastics which are processed at higher temperatures.

By using three different dispersing agents, PET/TiO_2 nanocomposites have been studied through their non-isothermal crystallization kinetics using differential scanning calorimetry (DSC), birefringence microscopy and thermo mechanical analysis (TMA).

The influence of TiO_2 nanoparticles and the different dispersing agents on PET non-isothermal crystallization behaviour is investigated using the Jeziorny's and Ozawa methods. Depending on the dispersing agent, TiO_2 nanoparticles act as nucleating or anti-nucleating agents in the PET crystallization process. The thermo mechanical analysis enabled to determine the beginning of glass transition and the intensity of this effect and the thermal stability of the composite that are modified by the nucleating or antinucleating behaviour of the filler.

EXPERIMENTAL PART

Materials

Poly(ethylene terephthalate) (PET) provided by ANTEX, S.L. 100% polyester (extra-bright), textile quality. PET pellets has been stored in a vacuum oven at 50°C and 80 mbar conditions to prevent the deterioration of the polymer by temperature and, with low pressure, avoiding the absorption of humidity of the sample.

Nanoparticles TiO_2 MT-100HD Tayca Corporation, provided by Zeus Química, S.A. Composition: TiO_2 80-98% (rutile), Al_2O_3 1-15%, ZrO_2 1-10%; particle size 15 nm; specific surface area = 75 m^2/g.

All the dispersants were supplied by Clariant and present the following properties:

Characteristics	Units	Target value		
		MAWMA	*PSEMA*	*AW*
Appearance		pale yellowish	yellowish	almost white powder
Acid value	[mg KOH/g]	15-20	10-14	max. 8
Drop point	[°C]	79-83ºC	96-102	139-144
Density (23°C)	[g/cm³]	~1.02	~1.02	~ 1.00

Esther of montanic acids with ethylene glycol or glycerine (MAWMA). Licowax OP differs in that the montanic acids are only partially esterified with butylene glycol, and the rest are saponified with calcium hydroxide. Therefore Licowax OP

Esther of montanic acids partly esterified with butylenes glycol and the rest saponified with calcium hydroxide (*PSEMA*) and that contains calcium montanate in addition to montanic acid esters, LICOWAX OP powder.

Amide wax based on N,N'-Bisstearylethylene-diamine (AW), LICOWAX C powder.

Sample preparation

The mixture PET/TiO_2 nanoparticles in the presence of the different dispersing agents was performed in a screw at 290°C and then extruded through a hole, at a screw speed of 70 rpm. The extruder was a Corima extruder Model G-132 A.

Substrates have been prepared without and with (3%) of TiO_2 nanoparticles in the presence and in the absence of the different dispersing agents (5%). Also a mixture of PET and TiO_2 without dispersing agent has been prepared.

Characterization

Kinetics of the non-isothermal crystallization

7.5 mg sample was introduced into alumina crucibles and was analyzed by a differential scanning calorimeter Perkin Elmer, model DSC7. Tests were performed with a nitrogen atmosphere (35ml·min^{-1}) using the following workflow:

1. Heating from 40°C to 290°C at a rate of 300°C/min.
2. Maintenance at 290°C for 4.5 min.
3. Cooling from 290°C to 40°C at cooling rates of 5, 10, 15 and 20°C/min.

Two measures of each sample were analyzed. The mean value and the confidential interval at 95% are included in results included in Tables 1 and 2.

Birefringence microscopy

Samples were prepared in the form of a plate in a 10T Bench Top Press, Rondol Technology. To do this, 10g of the substrate were placed in the press in a mould of 10x10x0.6 mm^3. Then, temperature was raised to 290°C, maintained for 5 min at a pressure of 60 kN and cooled. The prepared plates were studied in a Jenalab Pol U - DMC2 and observed under polarized light. The presence of bright "dots" indicates agglomeration of the nanoparticles.

Thermomechanical analysis (TMA)

Tests were carried out in a Mettler Toledo TMA/SDTA 840 between 25 and 200°C at a heating rate of 10°C/min. The purge gas is N_2 (g) at a rate of 35 ml/min. Pairs of rectangular specimens 5x15 mm were cut from plates prepared for birefringence microscopy, and were subjected to bending test by the application of a periodic load from 2.5 to 5 cN at 1/12 Hz. The TMA device for bending, the TMA plot and the most relevant parameters yielded by the analysis of the mean depletion curve, the E-storage component of Young's modulus and the Phase lag between the E-storage and E-loss components of the Young's modulus curves are shown in Figure 1. Two measures of each sample were analyzed. The mean value and the confidential interval at 95% are included in results included in Table 3.

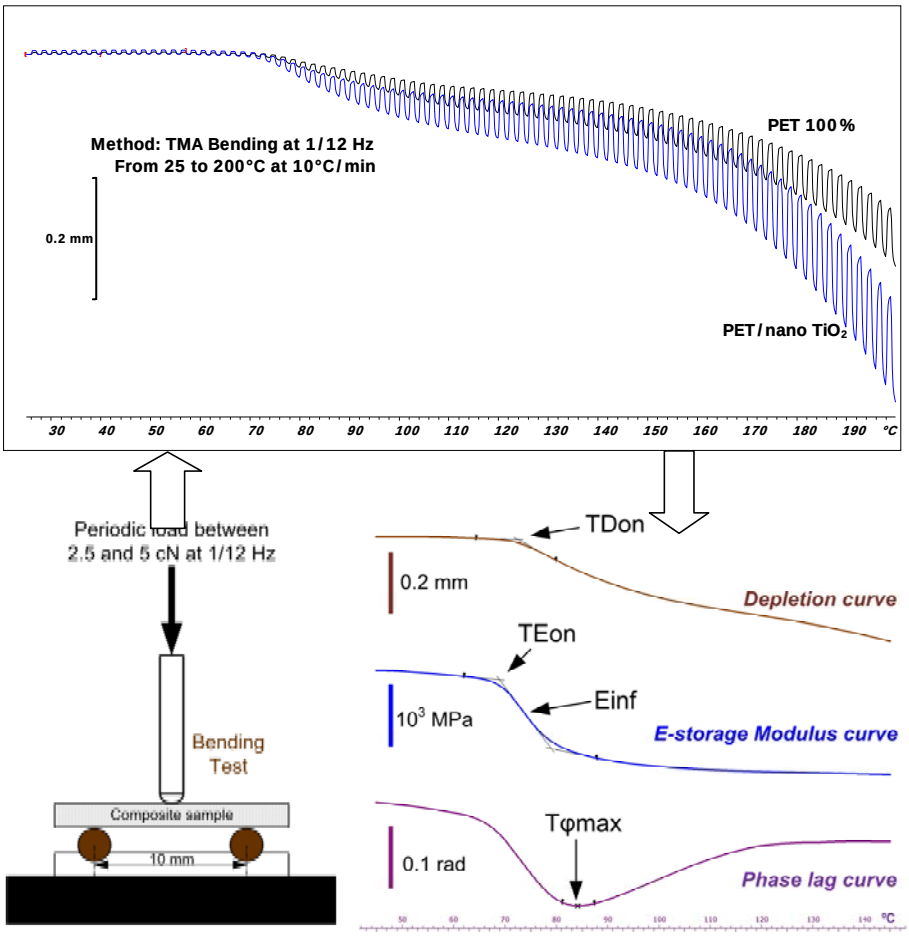

Figure 1. TMA bending device, TMA curves of PET and PET/TiO_2 nanocomposites from 25 to 200ºC and thermal transitions determined on the mean depletion, E-storage modulus and Phase lag curves: a) TDon (onset temperature of depletion), b) TEon (onset temperature of storage modulus fall) and Einf maximum slope of the E-storage fall at the inflection point, and c) Tφmax (temperature of maximum phase lag between E-loss and E-storage modulus curves.

- TDon: The onset temperature at which the composite sample begins to be irreversible bent (ºC).
- TEon: The onset temperature at which the E-storage modulus begins to fall (ºC).
- Einf: The maximum slope (falling rate) of the E-storage modulus (MPa/K).
- Tφmax: The temperature of maximum phase lag between E-loss and E-storage modulus curves (ºC).

RESULTS AND DISCUSION

Non-isothermal crystallization isotherms

The degree of conversion and the corresponding kinetic parameters were obtained from the thermograms obtained by DSC (Fig. 2) through the calculation of the partial areas of the exothermic crystallization peak (Eq.1).

$$\chi(t) = \frac{\int_0^t \left(\frac{dH}{dt}\right) dt}{\int_0^\infty \left(\frac{dH}{dt}\right) dt} = \frac{\Delta H_t}{\Delta H_\infty} \qquad \text{Eq. 1}$$

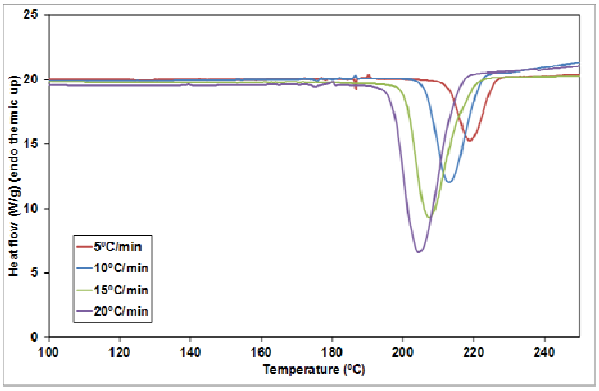

Figure 2. Thermograms of the non-isothermal crystallization of the sample containing *MAWMA* as dispersing agent.

The degree of crystallization at each cooling rate was determined by integrating the partial exotherm crystallization previously delimited. This delimitation was made by taking as reference time, t_o, the time at which crystallization begins.

Avrami method

The non-isothermal crystallization method calculates the evolution of the crystallinity in function of the

temperature at different constant cooling rates (Fig. 3a). From these data and taking into account that time and temperature are related by the cooling rate as indicated in equation 2, the growth of the increase in crystallinity in function of the time can be determined (Fig. 3b). The Avrami theory can be applied to these experiments using the model of isothermal crystallization modified by Jeziorny and described in Equation 3 [12-15], that relates the relative degree of crystallinity $\chi_t(T)$ at time t with the kinetic parameter Z_t, the Avrami crystallization rate constant, which is a function of the temperature and, in general depends on both the nucleation frequency and the crystal growth rate, and the Avrami kinetic exponent n which reflects the type of nucleation and/or the crystal growth morphology (1D, 2D or 3D) that depends on the crystallization mechanism [16].

$$(t - t_0) = \frac{T_0 - T}{v_c} \qquad \text{Eq. 2}$$

$$(1-\chi_t(T)) = exp\ (-Z_t\ t^n) \qquad \text{Eq. 3}$$

$$ln\left[-ln\left(1-\chi_t(T)\right)\right] = n\ lnt + lnZ_t \qquad \text{Eq. 4}$$

Fig 3, right, shows the evolution of the relative crystallinity (χ) with the time of the sample PET + TiO_2/*PSEMA* for the different cooling rates studied. This behaviour of the evolution of the relative crystallinity transformation in relation to time and temperature has been observed to be very similar in all the blends polymer/nanoparticle studied.

According to equation 3, representing $ln(-ln\ (1-\chi_t(T))$ vs. $ln\ t$ (Eq. 4), the kinetic parameters n and Z_t can be determined. Both are a diagnostic of the crystallization mechanism [17]. For the non-isothermal crystallization process, the Z_t estimated from Eq. 4 should be inadequate because of the influence of the cooling rate. Jeziorny [18] considerer that the parameter Z_t should be corrected as:

$$log\ Z_c = \frac{logZ_t}{\alpha} \qquad \text{Eq. 5}$$

where α is the cooling rate.

Fig. 4 shows the Avrami relation for substrates containing nanoparticles in the presence of the different dispersing agents in the experiment cooling at 10°C/min. Table 1 include the results of the crystallization temperature (Tc) and crystallization enthalpy (ΔH) obtained from Avrami kinetic analysis for the original polyester and its mixture with the different dispersing agents in the presence or in the absence of TiO_2 nanoparticles at different cooling rates. It is observed that the presence of *MAWMA* and *PSEMA* increases the crystallization temperature. That is, this dispersing agents act as nucleating agents. This nucleation occurs even at higher cooling rates temperatures in the presence of TiO_2. Nevertheless, *AW* dispersing agent decreases the crystallization temperature, being this decrease higher in the presence of TiO_2. That means that the properties of the ester of montanic acid compounds improve the nucleation properties of TiO_2 while amidic wax improves the anti-nucleation properties.

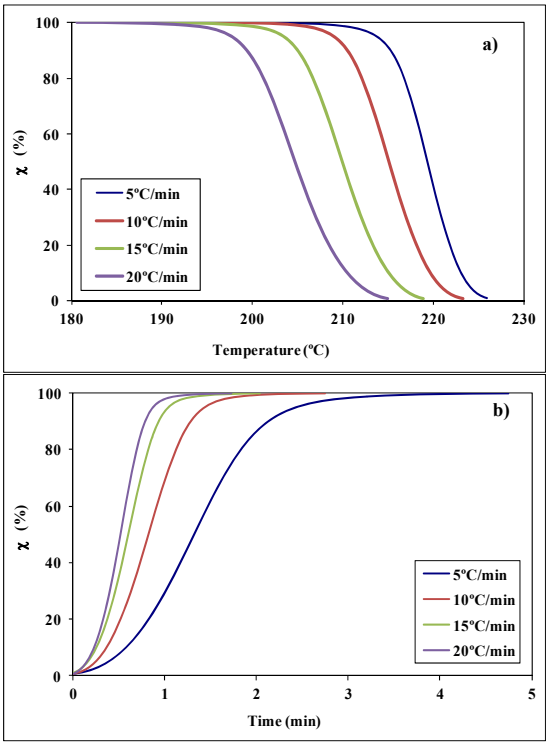

Fig. 3. Evolution of the relative crystallinity (χ) of the sample PET + TiO_2 + *PSEMA* dispersing agent for different cooling rates studied in function of temperature (left) or time (right).

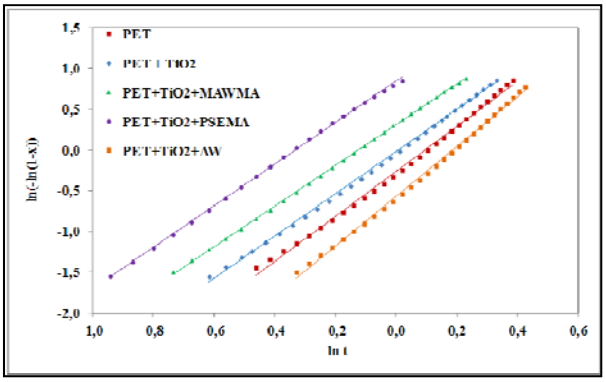

Fig. 4. Avrami relation for substrates containing TiO_2 and original PET.

The TiO_2 fillers may act as nucleating or anti-nucleating agent affecting the crystallization behaviour [19,20, 21]. TiO_2 nanoparticles have been described as nucleating agents in the PET crystallization. That is in accordance with the results obtained in the samples of PET/TiO_2 with *MAWMA* and *PSEMA* dispersing agents when compared with PET. Nevertheless, that does not agree with the results obtained with the amide wax. Taniguchi and Cakmak [22] described that the addition of TiO_2 nanoparticles could play the role of anti-nucleating agents during deformation from the amorphous precursors, by preventing the formation of

the crystalline nodes that eventually develop into three-dimensional network structures. They described that this phenomenon can be attributed to the disruption of strain induced crystallization process in the presence of particles that have poor surface interaction with the polymer at the rubbery temperature range. Following this interpretation, the mixture TiO_2/*AW* presents poor surface interaction with the polymer.

Table 1. Tc and ΔH obtained from Avrami kinetic analysis for the original polyester and its mixture with the different dispersing agents in the presence or in the absence of TiO_2 nanoparticles at different cooling rates (Mean values±95% C.I.).

Sample	*α* (ºC/min)	*Tc (ºC)*		*ΔH (J/g)*	
		0% TiO_2	3% TiO_2	0% TiO_2	3% TiO_2
PET	5	216.1±0.2	218.5±0.1	-56.1±4.5	-58.5±1.0
	10	211.0±0.3	212.6±0.5	-56.5±2.3	-56.5±2.2
	15	207.0±0.1	207.1±1.8	-57.3±0.3	-56.3±3.6
	20	202.5±0.3	203.7±0.1	-55.1±0.2	-54.9±3.4
PET + *MAWMA*	5	219.9±4.4	220.4±0.6	-52.2±0.5	-57.2±4.0
	10	215.5±0.3	216.0±0.1	-56.4±0.3	-57.1±2.4
	15	209.6±2.3	210.0±0.5	-55.9±0.3	-56.4±2.4
	20	205.8±1.0	206.8±1.0	-57.0±1.2	-57.6±1.0
PET + *PSEMA*	5	221.2±1.8	220.7±2.8	-57.1±4.4	-57.7±0.8
	10	214.2±0.2	215.7±1.3	-56.9±1.4	-58.2±6.2
	15	209.1±1.3	210.1±0.8	-56.3±2.3	-57.9±0.3
	20	204.5±2.3	204.2±0.3	-56.2±3.1	-57.7±2.3
PET + *AW*	5	219.4±0.1	216.80±0.1	-53.5±0.1	-57.3±2.2
	10	211.9±0.2	208.8±0.3	-56.6±0.3	-57.9±1.5
	15	204.4±0.3	203.5±1.0	-56.0±1.0	-56.1±0.7
	20	200.8±2.1	200.0±0.1	-50.9±2.5	-58.4±0.1

Table 2. Zc, n and $t^{1/2}$ obtained from Avrami kinetic analysis for the original polyester and its mixture with the different dispersing agents in the presence or in the absence of TiO_2 nanoparticles at different cooling rates (Mean values±95% C.I.).

Sample	α (ºC/min)	Zc (min^{-n})		n		$t^{1/2}$ (min)	
		0% TiO_2	3% TiO_2	0% TiO_2	3% TiO_2	0% TiO_2	3% TiO_2
PET	5	0.74±0.09	0.78±0.01	2.75±0.37	2.54±0.04	1.44±0.01	1.43±0.03
	10	0.98±0.01	0.98±0.03	2.98±0.10	2.85±0.35	0.96±0.01	0.96±0.10
	15	1.06±0.01	1.05±0.01	2.90±0.05	2.86±0.14	0.68±0.01	0.71±0.04
	20	1.07±0.01	1.06±0.01	3.04±0.7	2.95±0.28	0.59±0.06	0.60±0.06
PET + *MAWMA*	5	0.72±0.03	0.74±0.09	2.79±0.07	2.79±0.13	1.60±0.11	1.36±0.08
	10	1.04±0.01	1.03±0.01	2.57±0.02	2.44±0.08	0.76±0.01	0.76±0.01
	15	1.07±0.01	1.07±0.01	2.73±0.11	2.69±0.14	0.61±0.05	0.59±0.02
	20	1.08±0.01	1.08±0.01	2.78±0.13	2.66±0.01	0.50±0.03	0.50±0.01
PET + *PSEMA*	5	0.82±0.01	0.84±0.04	2.51±0.10	2.45±0.07	1.31±0.03	1.23±0.25
	10	1.02±0.0	1.06±0.05	2.60±0.05	2.57±0.03	0.81±0.02	0.72±0.27
	15	1.07±0.01	1.07±0.01	2.79±0.15	2.58±0.02	0.63±0.01	0.59±0.01
	20	1.07±0.01	1.07±0.01	2.90±0.17	2.67±0.03	0.56±0.02	0.52±0.08
PET + *AW*	5	0.68±0.02	0.64±0.01	3.00±0.02	3.11±0.04	1.69±0.07	1.84±0.02
	10	0.98±0.01	0.95±0.01	2.74±0.02	3.08±0.02	0.94±0.02	1.08±0.01
	15	1.04±0.01	1.02±0.0	3.02±0.06	2.94±0.14	0.73±0.01	0.80±0.01
	20	1.06±0.02	1.05±0.01	2.88±0.26	2.48±0.27	0.61±0.11	0.59±0.12

About crystallinity enthalpy, it is not significantly modified by the presence of the different dispersing agents, neither by the increase of the nanoparticles as observed by the small variations in crystallization enthalpy ΔH_c. Results of ΔH_c have been calculated taking into account the actual concentration of nanoparticles as follows:

$$\Delta H_c = \frac{\Delta H_{exp}}{w} \qquad \text{Eq. 6}$$

where ΔH_c is the crystallization enthalpy of the polyester in the mixture

ΔH_{exp} is the enthalpy of crystallization of the sample, and

w is the percentage of polyester in the mixture.

The Avrami kinetic parameter, n, remains approximately constant, regardless of the cooling rate, the dispersing agent and the concentration of nanoparticles. The value of n is 2.77 (±0.19), demonstrating that the nucleation which occurs is heterogeneous in the form of spherulites in three dimensions.

Z_t increases with the cooling rate since the crystallization occurs more quickly at lower temperatures [23]. Z_c parameter has been calculated by Eq. 5 to avoid the influence of cooling rate in this parameter. Although theoretically Z_c is not dependent of cooling rate, this affirmation is almost true for cooling rates higher than 5ºC/min, being Zc at this cooling rate of 0.74±0.06 and presenting a mean value of 1.05±0.03 for cooling rates of 10, 15 and 20ºC/min respectively.

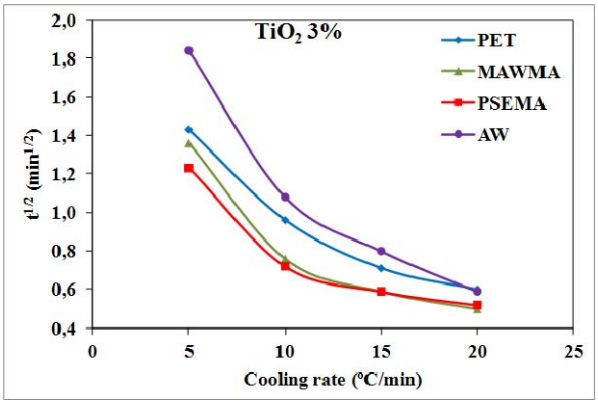

Fig. 5. Relation between half crystallization time and cooling rate in the presence and in the absence of TiO_2.

Half crystallization time for all the substrates is represented in Fig. 5. No differences in the half crystallization time in the case of PET without dispersing agent in the absence or presence of TiO_2 were observed. In the presence of *MAWMA* and *PSEMA* additives, half crystallization times are smaller than without dispersing agent and, when TiO_2 is added, the reaction is faster particularly for short cooling rates. This confirms the nucleating action of these products. However, the half crystallization time in the presence of AW is less than in the case of original polyester, confirming its anti-nucleating action.

Another important parameter is the determination of the dispersing effect of the different additives. When aggregated, nanoparticles present dimensions that could be visible by optical microscopy by birefringence method due to the fact that crystals present bright dots in the prepared substrate. From results (Fig. 6), substrates without dispersing agent and with *PSEMA* (a and c, respectively) present agglomeration dots. On the other hand, *MAWMA and AW* seem to be good dispersing agents for the studied nanoparticles.

When the results of crystallization temperature and half-crystallization time given by the Avrami kinetic analysis and the birefringence method of the optical microscopy are considered, the best nucleating and dispersing properties can be attributed to the ester of montanic acids with multifunctional alcohols *(MAWMA)*.

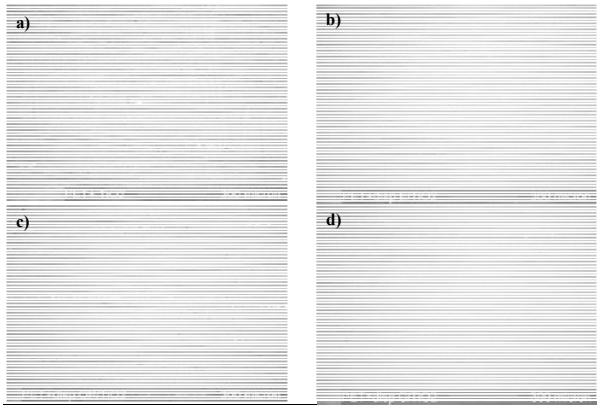

Fig. 6. Birefringence microscopy of substrates containing 3% TiO_2. a) without dispersing agent, b) with *MAWMA*, c) with *PSEMA* and d) with *AW*.

Thermomechanical analysis

Figure 1 shows the TMA plot of a PET100% sheet and that of a nano TiO_2/PET composite without any dispersing agent. As regards the temperature at which the mean depletion curve begins to be irreversible bent TDon, the inclusion of nanoparticles makes this temperature to be decreased from 73.8 to 71.4ºC. The same occurs with the onset temperature at which the E-storage component of the Young's modulus begins to fall: it descends from 70.3 to 67.7ºC. Otherwise the inclusion of nanoparticles makes the maximum phase lag temperature Tφmax, where the mobility of the amorphous phase reaches its maximum, to ascend. These observations enabled us to consider that the inclusion of nanoparticles increases the range of the glass transition region that can be related with an increase in the heterogeneity of the linkages between the matrix chains, distorted by the presence of the TiO_2 nano particles. The result is in accordance with the lower fall rate of the Young's modulus curve (Einf) that decreases from 142.5 to 93.9 MPa/K when nanoparticles are included. The presence of nanoparticles makes the glass transition begin at lower temperatures and increases its range which can be related with the absence of a nucleating effect of the nanoparticles when included into the polymer [24]. The poor interaction between nanoparticles and polymer makes the former to act as a plasticiser favouring the mobility of polymer chains. The broadness of the glass transition region could also be influenced by the plasticizers [25].

Figure 7 shows the TMA curves of the PET samples without and with a 5% of the three dispersing agents.

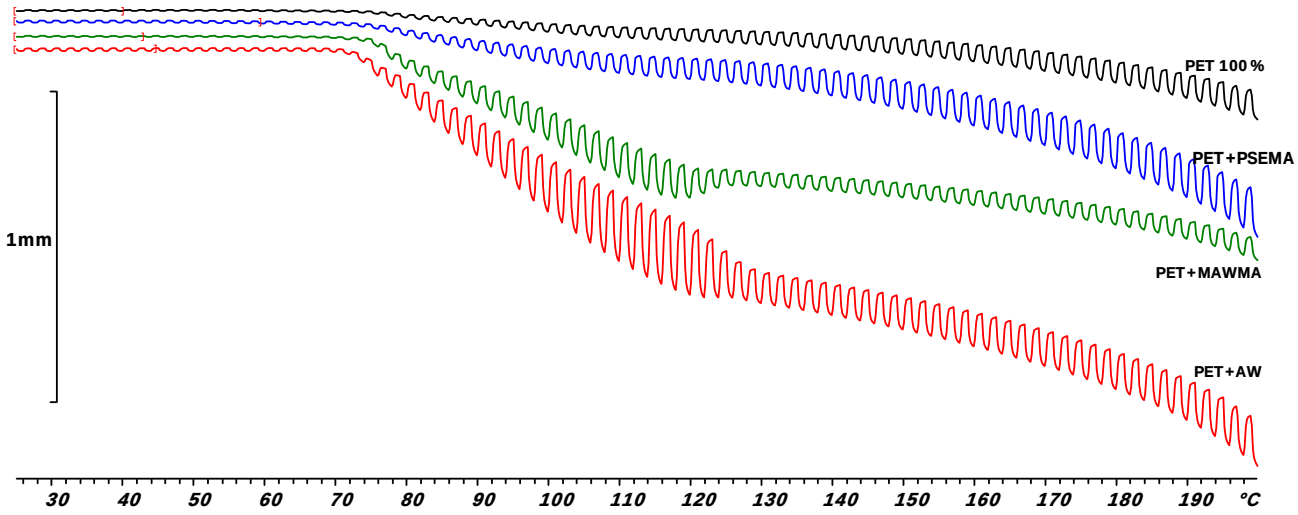

Fig. 7. TMA curves of PET and PET/dispersing agents without TiO_2 nanoparticles.

The inclusion of PSEMA in PET makes the TMA curve approaching to that of the PET/TiO_2 nanoparticles (cfr. Fig. 1), while those of the PET/MAWMA and PET/AW blends show a different plot. Along the glass transition region a progressive and sustained growth increase in mobility of PET chains is observed up to approximately 120ºC, where a rather sudden thermal stability is reached. MAWMA is the dispersing agent that leads to the lowest amplitude in deformation and bias with temperature up to 200ºC. The decrease in amplitude of the TMA curve is caused by an ascend in the Young's modulus due to the growth in size and perfection of crystals favoured by the higher mobility of polymer chains in accordance with the flow properties claimed by Clariant to this dispersing agent when included in PET.

Table 3. Onset temperature of irreversible bending of the mean depletion curve TDon, onset temperature of E-storage modulus fall TEon, maximum fall rate of the E-storage curve and maximum Phase lag between E-loss and E-storage modulus given by the thermomechanical analysis (Mean values±95% C.I.).

Sample	TDon (ºC)	TEon (ºC)	Einf (MPa/K)	Tφmax (ºC)
PET	73.8±1.7	70.3±0.9	-142.5±19.3	79.9±1.9
PET+TiO_2	71.4±1.7	67.7±0.9	-93.9±19.3	82.1±1.9
PET+TiO_2/AW	69.7±1.7	66.6±0.9	-113.3±19.3	82.8±1.9
PET+TiO_2/MAWMA	72.2±1.7	67.9±0.9	-87.6±19.3	83.2±1.9
PET+TiO_2/PSEMA	70.5±1.7	66.9±0.9	-111.1±19.3	81.7±1.9

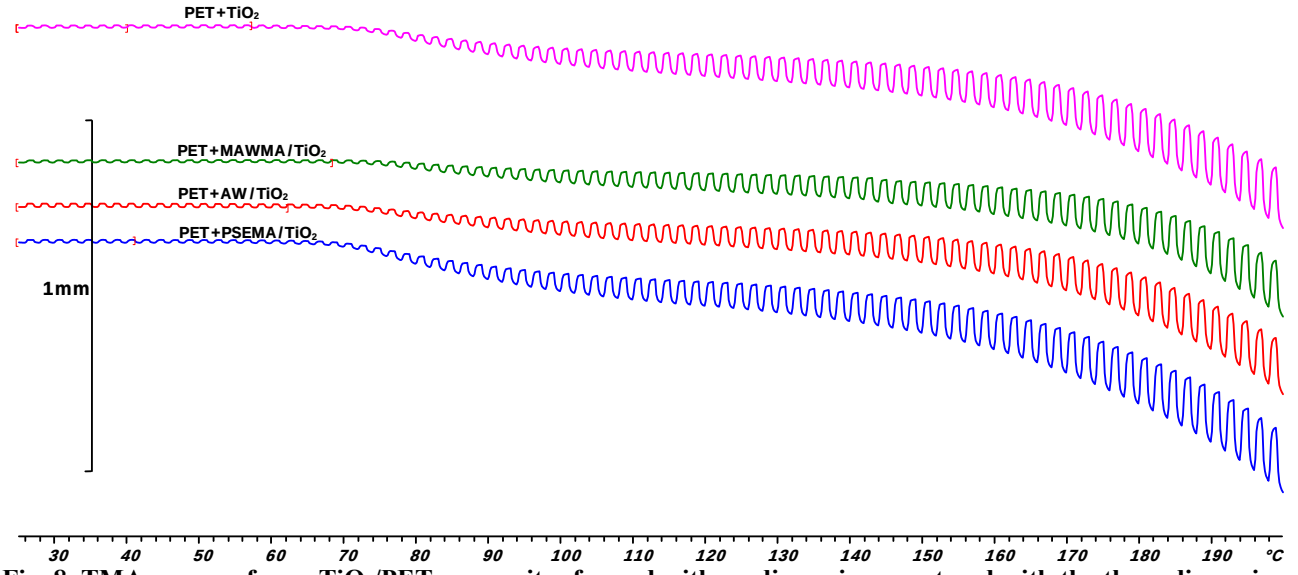

Fig. 8. TMA curves of nanoTiO_2/PET composites formed with no dispersing agent and with the three dispersing agents.

Figure 8 shows the TMA curves of PET/TiO_2 nanocomposites without and with the three different dispersing agents. The amplitude and bias of the TMA curves along the test makes evident the improvement in thermal stability caused by the inclusion of dispersing agents. The nucleating effect can be associated with an increase in the onset temperature of the glass transition that can be dimensionally measured by the onset temperature of the depletion curve TDon, or mechanically determined by the onset temperature of the E-storage modulus fall TEon. Normally the increase in onset temperatures are linked to lower fall in the E-storage at the inflection point of the curve (Einf) and higher temperatures to reach the highest mobility of the amorphous fraction, caused by better size and perfection of crystals favoured by the nucleating effect of the filler. Table 3 shows that *MAWMA* increases the onset temperatures of the depletion and E-storage and maximum phase lag curves, while decreases the maximum fall rate of the E-storage when compared with that of the composite without dispersing agent. Consequently the results confirms *MAWMA* as the dispersing agent that makes the TiO_2 nanoparticles shows the best nucleating characteristics when included in PET.

CONCLUSIONS

As regards the study of the effect of different dispersing agents based on montanic and amide waxes on the nucleating effect of TiO_2 nanoparticles for PET/TiO_2 nanocomposites production, the following conclusions are obtained:

The non-isothermal crystallization using the Avrami method, enabled to determine an increase in the crystallization temperature when an ester of montanic acid with multifunctional alcohols (*MAWMA*) and a partly saponified ester of montanic acid (*PSEMA*) is used, while the amide wax base on N,N'-bisstearoyl ethylenediamine (*AW*) decreases the crystallization temperature in presence of TiO_2. This means that the properties of the ester of montanic acid compounds improve the nucleation properties of TiO_2 while the amidic wax improves the anti-nucleation properties. The half crystallization time with *MAWMA* and *PSEMA* were smaller than those yielded without dispersing agent, confirming the nucleating effect action of these components.

The birefringence microscopy confirms the good dispersing characteristics of TiO_2 nanoparticles in PET of *MAWMA* and *AW*.

The thermomechanical analysis confirms the influence of *MAWMA* on the nucleating effect of TiO_2 nanoparticles in PET, because leads to the highest increase in the onset temperatures of glass transition, the maximum phase lag temperature, shortening the fall in the E-storage modulus along the glass transition region. This confirms its best capacity to promote the nucleating effect of TiO_2 nanoparticles when included in PET.

In summary, among the studied waxes, the ester of montanic acids with multifunctional alcohols *(MAWMA)* presents the best nucleating and dispersing properties of TiO_2 nanoparticles when included in PET.

Acknowledgements

We gratefully acknowledge the financial support for this research from the Ministry of Science and Innovation of Spain (Project MAT2010-20324-CO2). Also, we would like to thank the companies Anglés Textil, S.A., Zeus Química, S.A. and Clariant for providing polyester pellets, TiO_2 nanoparticles and dispersing agents, respectively.

Finally, we acknowledge Mrs. Carmen Escamilla and Mrs. Montserrat García for their support in the experimental work.

References

1. Additivi ceramici per le fiber tessili, Nuove Fiber, 10 September 2001 (on line journal, last access April 2015, http://www.technica.net/NF/Caratteristiche_&_Prestazioni/additivi.htm)
2. Keqing, H., Muhuo, Y. (2006) J. Appl. Polym. Sci., 100, 1588.
3. Juangvanich, N., Mauritz, K. A. (1998) J. Appl. Polym. Sci., 67, 1799.
4. McNally, T., Murphy, R. W., Lew, Y. C., Turner, J. R., Brennan, P. G. (2003) Polymer, 44, 2761.
5. Lantelme, B., Dumon, M., Mai, C., Pascault, J. P. (1996) J. Non-Crystalline Solids, 194, 1-2, 63.
6. Li, Y., Yu, J., Guo, Z. (2003) Polym. Int., 52, 981.
7. Chang, J., Kim, S. (2004) Polymer. 45, 919.
8. Shen, L., Du, Q., Wang, H., Zhong, W., Yang, Y. (2004) Polym. Int., 53, 1153.
9. Neouze, M. A., Schubert, U. (2008) Monatshefte für Chemie Chemical Monthly, 139, 183.
10. Cayuela, D., Cot, M., Riva, M., Sanchez, R. J., Sánchez-Loredo, M. G., Algaba, I, Manich, A. M. (2014) Journal of Macromolecular Science, Part A: Pure and Applied Chemistry, 51, 831.
11. Clariant International Ltd., Technical brochure "Lubricants for plastic processing", Document DA 8274 E, 05.2013.
12. Avrami, M., J. Chem. Phys., 7, 1103 (1939).
13. Avrami, M., J. Chem. Phys., 8, 212 (1940).
14. Avrami, M., J. Chem. Phys., 9, 177 (1941).
15. Jeziorny, A. (1978) Polymer, 19, 1142.
16. Vyazovkin, S., Sbirrazzuoli, N. (2003) J. Phys. Chem. B, 107, 882-888.
17. Jiang, C., Wang, D., Zhang, M., Li, P., Zhao, S. (2010) European Polymer Journal, 46, 2206.
18. Jeziorny A. (1978) Polymer, 19(10), 1142.
19. Xiuling, Z., Biao, W., Shiyan, C., Chaosheng, W., Yumei, Z., Huaping, W. (2008) Journal of Macromolecular Science - Part B. Physics, 47, 1117.
20. George, Z. P., Dimitris, S.A., Dimitris, N.B., George, P. K. (2005) Thermochim. Acta., 427, 117.
21. Kotek, J., Kelnar, I., Baldrian, J., Raab, M. (2004) Euro. Polym. J., 40, 679.

22. Taniguchi, A., Cakmak, M. (2004) Polymer, 45, 6647.
23. Pérez, C. J., Alvarez, V. A. (2009) Journal of Applied Polymer Science, 114, 3248.
24. Debenedetti, P.G., Stillinger, F.H. (2001) Nature, 410, 259.
25. Xu, B., McKenna, G.B. (2011) J. Chem. Phys., 134, 124902